



Enhancement of the diffraction efficiency of the hologram recorded in photorefractive media under the action of external electric field

T.K. Yadav, M.K. Maurya, R.A. Yadav*

Laser and Spectroscopy Laboratory Department of Physics, Banaras Hindu University, Varanasi 221005, India

ARTICLE INFO

Article history:

Received 28 January 2011

Accepted 1 July 2011

Keywords:

Photorefractive materials

Diffraction efficiency

Diffusion field and reduced fringe contrast

modulation ratio of the index grating

ABSTRACT

Diffraction efficiency as a function of the applied electric field for the non-linear regime has been calculated by solving numerically the beam coupling equations. The refractive index variation used in the beam coupling equations was calculated directly from the material rate equations via the total space charge field. The diffraction efficiency of the holograms recorded in photorefractive media is not only a function of the applied external electric field but also a function of crystal thickness, diffusion field, reduced fringe contrast modulation ratio and absorption coefficient of the materials. The effects of these parameters on the efficiency of the holograms have been studied in details. In the absence of the external applied field, it is found that the diffraction efficiency of the holograms could be maximized for a thinner photorefractive crystal having lower absorption coefficient and higher value of diffusion field, which could exist at a much lower value of reduced fringe contrast modulation ratio of the index grating. More efficient holograms can be recorded in the presence of the externally applied electric field as compared to the case of no external field.

© 2011 Elsevier GmbH. All rights reserved.

1. Introduction

Photorefractive materials are of considerable research interest for the development of optical devices [1], e.g. image processing, real-time holography, optical information storage, and optical phase conjugation. Application of externally applied electric field has been found to enhance many of the desired properties of these materials, such as diffraction efficiency [2], photorefractive response time [3], and holographic storage capacity [4]. The photorefractive effect appears in materials which exhibit an electric field dependent refractive index and are photosensitive, such that the spatial distribution of photo-generated charge carriers is modified on irradiation with light. The diffraction pattern formed by the interference of two coherent light beams within such materials generates a non-uniform internal electric field that in turn modulates the refractive index. The resulting refractive index pattern forms a grating which can diffract light and thereby give rise to two beam coupling, whereby one of the writing beams gains energy at the expense of the other – a property that can be exploited in photonic devices. A detailed study of several electric-field related effects in photorefractive crystals, such as amplitude and phase coupling, linear and nonlinear electro-optic effects, and the piezoelectric effect was conducted by De Vre et al. [5]. Hologram multiplexing has been demonstrated in photorefractive crystals

with a variable electric field used to control the Bragg condition [6,7].

Much innovative geometry have been proposed by various group of workers to record holograms in these photorefractive media with and without externally applied electric field across the crystal in both the two and four-wave mixing geometries [8–10]. Also, to implement photorefractive holographic interferometry in an industrial environment one must need highly efficient holograms in real-time. One of the solutions to increase the diffraction efficiency of the photorefractive holograms is the application of electric field and magnetic field across the crystal [11–13]. But it may be cumbersome to implement such techniques in the industrial environment. Later, a new real-time photorefractive holographic technique using two-wave mixing geometry by exploiting the anisotropic self-diffraction geometry was proposed by Kamshilin et al. [14] using BTO, which was then implemented using BSO with higher diffraction efficiency by Troth and Dainty [15]. These two dynamic holograms had good efficiency without the externally applied electric field and the main advantage was that one can use polarizer and analyzer pair to separate out diffracted beams. In fact, this two-wave mixing and anisotropic diffraction geometry was very suitable to dynamic holographic interferometry. Again in this case also the diffraction efficiency of the holograms is about 30% for BSO and much less for BTO. Therefore, it becomes necessary to develop a new technique to improve the diffraction efficiency of the holograms recorded in these photorefractive media with the weak external applied field.

* Corresponding author.

E-mail addresses: rayadav@bhu.ac.in, ray1357@gmail.com (R.A. Yadav).

In the present paper we propose new geometry to record more efficient holograms in the photorefractive media (e.g. BaTiO₃) with the weak external applied field using the phase conjugate beam of the signal beam itself act as other writing beam. The advantage of this geometry is that more efficient holograms can be recorded at very low applied electric field (~1 kV/cm) which is significantly less than that reported in literature (20 kV/cm) [16]. The diffraction efficiency of the holograms recorded in photorefractive media is not only a function of the externally applied electric field but also a functions of crystal thickness, diffusion field, reduced fringe contrast modulation ratio and absorption coefficient of the materials. The effects of these parameters on the efficiency of the holograms have been studied in details for the first time.

2. Mathematical description

The electric fields of the signal beam (E_s) and conjugate of the signal beam (E_{cs}) are given by,

$$E_s = A_s \exp[i(\vec{K} \cdot \vec{r} - \omega t)] \tag{1}$$

$$E_{cs} = A_{cs} \exp[-i(\vec{K} \cdot \vec{r} - \omega t)] \tag{2}$$

where A_s and A_{cs} are the amplitudes of the signal beam and conjugate of the signal beam, respectively, \vec{K} is the grating wave vector, ω is the frequency of the beams and \vec{r} and t are the space and time coordinates while propagating through the photorefractive crystal, these waves interfere and give rise to the resultant intensity I as,

$$I = I_0 [1 + \beta \cos(2\vec{k}_g \cdot \vec{x})] \tag{3}$$

where $I_0 = I_s + I_{cs}$ is the sum of the intensities of the two beams, k_g is the magnitude of the grating wave vector, $I_s = |A_s|^2$, $I_{cs} = |A_{cs}|^2$ are the signal beam intensity and conjugate signal beam intensity. β is the grating modulation depth given by,

$$\beta = \frac{2\sqrt{I_g I_{cs}}}{I_g + I_{cs}} = \frac{2\sqrt{M}}{1 + M}$$

with the parameter M (the intensity ratio of the two beams) defined by,

$$M = \frac{I_{cs}}{I_g} \tag{4}$$

If N_D and N_D^i be densities of neutral and ionized donor impurity, the net generation rate of electrons N_e is given by the difference between the rates of generation of electrons from the donors level and recombination of electrons to the donor level, and is equal to,

$$N_e = (\beta_T + sI) (N_D - N_D^i) - \gamma_R N N_D^i \tag{5}$$

where s is the photo-excitation cross-section, γ_R is the electron ionized recombination constant, β_T is the thermal excitation rate of electrons and N is the concentration of electrons in the conduction band. Neglecting the thermal generation (i.e. $\beta_T \ll sI$) the net generation of the electrons can be written as,

$$N_e = sI(N_D - N_D^i) - \gamma_R N N_D^i \tag{6}$$

The factors responsible for the motion of electrons in the conduction band are: (i) diffusion force due to incident spatially modulated light intensity from the regions of higher concentration to the regions of lower concentration, (ii) drift force due to an externally applied electric field and (iii) due to photovoltaic effect. Therefore, the total current density J can be written as,

$$J = J_{DR} + J_{Diff} + J_{p_v} \tag{7}$$

where

$$J_{DR} = e\mu NE \tag{8a}$$

$$J_{Diff} = \mu k_B T \frac{\partial n}{\partial x} \tag{8b}$$

$$J_{p_v} = p_v(N_D - N_D^i)I \tag{8c}$$

Eqs. (7) and (8a)–(8c) yield,

$$J = e\mu NE + \mu k_B T \frac{\partial n}{\partial x} + p_v(N_D - N_D^i)I \tag{9}$$

where μ is the electron mobility, p_v is the photovoltaic constant, E is the electric field, e is the electronic charge, k_B is the Boltzmann constant and T is the temperature. Combining Eqs. (5) and (9) in continuity equations, one can write the rate equation for the electron concentration in the conduction band as,

$$\frac{\partial N}{\partial t} = N_e + \frac{1}{e} \frac{\partial J}{\partial x} \tag{10}$$

Similarly, the continuity equation for the density of ionized donors can be written as

$$\frac{\partial N_D^i}{\partial t} = N_e \tag{11}$$

The electric field in the crystal is given by one dimensional (along the x -axis) Poisson's equation,

$$\frac{\partial E}{\partial x} = \frac{e}{\epsilon_s} (N_D^i - N_A^i - N) \tag{12}$$

where ϵ_s is the static dielectric permittivity (independent of position) and N_A^i is the density of ionized acceptor. For the steady state case the electrostatic condition implies that,

$$\vec{\nabla} \times \vec{E} = 0 \tag{13}$$

And also assuming that $N \ll N_A$, $N_D - N_A$, $N_D^i \approx N_A$ and after a few steps of algebraic manipulation the equation for the number of free electron takes the form,

$$N = N_0 [1 + m \cos(2\vec{k}_g \cdot \vec{x})] \tag{14}$$

where $N_0 = g(I_0)\tau_R$, $g(I_0)$ is the linear generation rate and τ_R is the life-time of free electrons. Here, m is the reduced fringe contrast modulation ratio given by,

$$m = \frac{M}{[1 + (\beta/sI_0)]} \tag{15}$$

Integration of Eq. (12) gives the electric field component E_x (along the x -axis) as,

$$E_x = \frac{(J - eD(\partial N/\partial x))}{e\mu N} \tag{16}$$

where, $D = \mu k_B T/e$ is the diffusion coefficient.

Eqs. (6), (14) and (16) yield,

$$E = \frac{J}{e\mu N_0} \cdot \frac{1}{1 + m \cos(2\vec{k}_g \cdot \vec{x})} - \frac{D\vec{k}_g}{\mu} \cdot \frac{2m \sin(2\vec{k}_g \cdot \vec{x})}{1 + m \cos(2\vec{k}_g \cdot \vec{x})} \tag{17}$$

For a boundary condition of constant applied voltage V over a material of length L , we must have

$$\frac{1}{L} \int_0^L E \, dx = \frac{V}{L} = \frac{J}{e\mu N_0} \frac{1}{L} \int_0^L \frac{1}{1 + m \cos(2\vec{k}_g \cdot \vec{x})} \, dx - \frac{D\vec{k}_g}{\mu} \frac{1}{L} \times \int_0^L \frac{2m \sin(2\vec{k}_g \cdot \vec{x})}{1 + m \cos(2\vec{k}_g \cdot \vec{x})} \, dx \tag{18}$$

For a large number of fringes in the crystal length (L) one can write,

$$\frac{1}{L} \int_0^L \frac{1}{1 + m \cos(2\vec{k}_g \cdot \vec{x})} \, dx = \frac{1}{2\sqrt{1 - m^2}}$$

$$\frac{1}{L} \int_0^L \frac{2m \sin(2\vec{k}_g \cdot \vec{x})}{1 + m \cos(2\vec{k}_g \cdot \vec{x})} dx = 0 \tag{19}$$

which implies that,

$$J = 2\sqrt{(1 - m^2)\sigma_0 E_a} \tag{20}$$

$$\sigma_0 = e\mu N_0 \tag{21}$$

where $E_a = V/L$ is the magnitude of the externally applied electric field.

It may be noted that for the applied electric field, the conductivity of co-sinusoidal illumination is reduced by a factor $2\sqrt{(1 - m^2)}$ related to the conductivity σ_0 for uniform illumination at the same average intensity [17]. Eq. (17) can also be written as,

$$E = E_a \cdot \frac{2\sqrt{(1 - m^2)}}{1 + m \cos(2\vec{k}_g \cdot \vec{x})} - E_d \cdot \frac{2m \sin(2\vec{k}_g \cdot \vec{x})}{1 + m \cos(2\vec{k}_g \cdot \vec{x})} \tag{22}$$

Eq. (22) consists of two parts, the first part represents the field due to drift and the second part is the field due to the diffusion. Here E_d is known as the characteristic field and is given by,

$$E_d = \frac{D\vec{k}_g}{\mu} = \left(\frac{k_B T}{e}\right) k_g \tag{23}$$

The characteristic field is independent of the material properties and depends on the temperature only. In the absence of an externally applied electric field the charge is migrated due to diffusion only and Eq. (22) reduces to,

$$E = -E_d \cdot \frac{2m \sin(2\vec{k}_g \cdot \vec{x})}{1 + m \cos(2\vec{k}_g \cdot \vec{x})} \tag{24}$$

Eq. (24) is the space-charge field (SCF) (for diffusion alone) and is denoted by E_{sc} . In photorefractive materials the SCF plays an important role and is created by two different mechanisms: (i) the drift (due to the applied field) and (ii) the diffusion (independent of the applied field). The SCF which is created due to charge separation introduces a change in the refractive index via the linear electro-optic effect (Pockels effect), is given by [18,19],

$$\Delta n = \frac{1}{2} n_r^3 r_{eff} E_{sc} \tag{25}$$

where Δn is the change in refractive index, r_{eff} is the effective electro-optic coefficient and n_r is the unperturbed refractive index. This change in the refractive index leads to a refractive index grating and the diffraction efficiency (η) of such a grating is given by [20,21],

$$\eta = \exp\left(-\frac{\alpha l}{\cos \theta_B}\right) \cdot \sin^2\left(\frac{\pi l}{\lambda \cos \theta_B} \Delta n\right) \tag{26}$$

Using Eqs. (24)–(26) the diffraction efficiency (η) takes the form

$$\eta = \exp\left(-\frac{\alpha l}{\cos \theta_B}\right) \cdot \sin^2\left(\frac{1}{2} n_r^3 r_{eff} E_d \cdot \frac{\pi l}{\lambda \cos \theta_B} \cdot \frac{2m \sin(2\vec{k}_g \cdot \vec{x})}{1 + m \cos(2\vec{k}_g \cdot \vec{x})}\right) \tag{27}$$

Eq. (27) represents the diffraction efficiency of the index grating without the externally applied field. In the presence of an externally applied electric field of magnitude E_a the diffraction efficiency of the index grating takes the form,

$$\eta = \exp\left(-\frac{\alpha l}{\cos \theta_B}\right) \cdot \sin^2\left(\frac{\pi l}{\lambda \cos \theta_B} \frac{1}{2} n_r^3 r_{eff} \cdot \left\{ E_a \cdot \frac{2\sqrt{(1 - m^2)}}{1 + m \cos(2\vec{k}_g \cdot \vec{x})} - E_d \cdot \frac{2m \sin(2\vec{k}_g \cdot \vec{x})}{1 + m \cos(2\vec{k}_g \cdot \vec{x})} \right\}\right) \tag{28}$$

Eq. (28) represents the expression for the diffraction efficiency of the index grating as a function of the externally applied electric field.

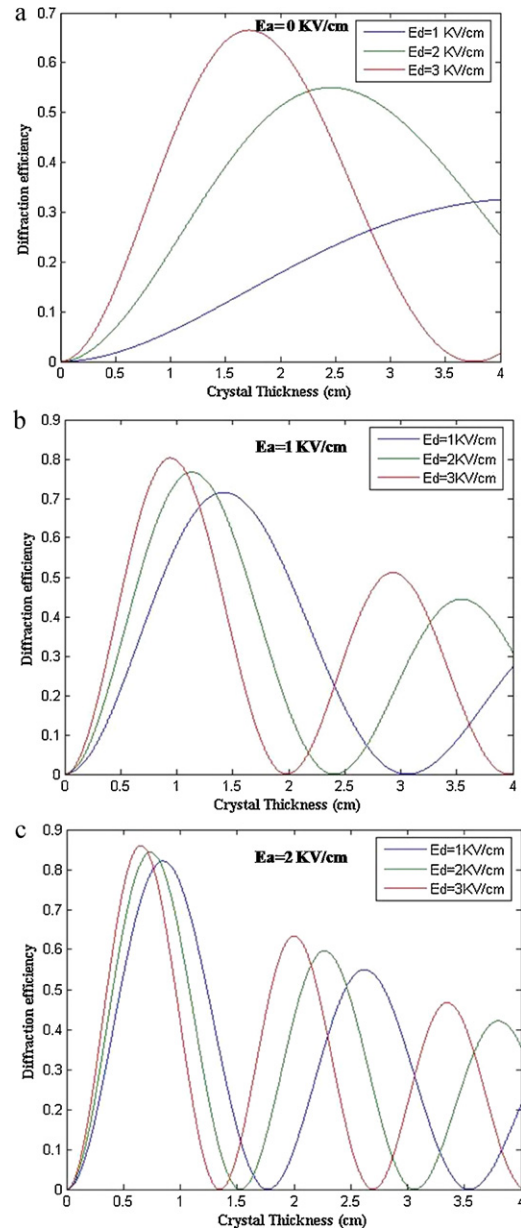


Fig. 1. Variation of diffraction efficiency with crystal thickness for different values of diffusion field with and without applied electric field.

3. Result and discussion

From Eq. (28) it is clear that the diffraction efficiency is a function of diffusion field, externally applied electric field, reduced fringe contrast modulation ratio, crystal thickness and absorption coefficient of the photorefractive material. Variation of diffraction efficiency with the crystal thickness (for $m=0.8$, $\theta_B = 28^\circ$, $K_g \cdot x = 3$, $\alpha = 0.2 \text{ cm}^{-1}$, $\lambda = 632.8 \text{ nm}$, $n_r = 2.41$, $r_{eff} = 28 \times 10^{-10} \text{ cm/V}$) for different values of diffusion field are shown in Fig. 1(a)–(c). From these figures it is evident that the diffraction efficiency of the refractive index grating varies periodically with the crystal thickness like a damped harmonic oscillation. In this case the absorption of the material plays the role of the damping force in the diffraction grating. The diffraction efficiency of the refractive index grating is found to be higher for the higher value of diffusion field and maximum diffraction efficiency can be achieved in thin photorefractive material provided the diffusion field of the materials is more than 2 kV/cm. The diffraction efficiency can be

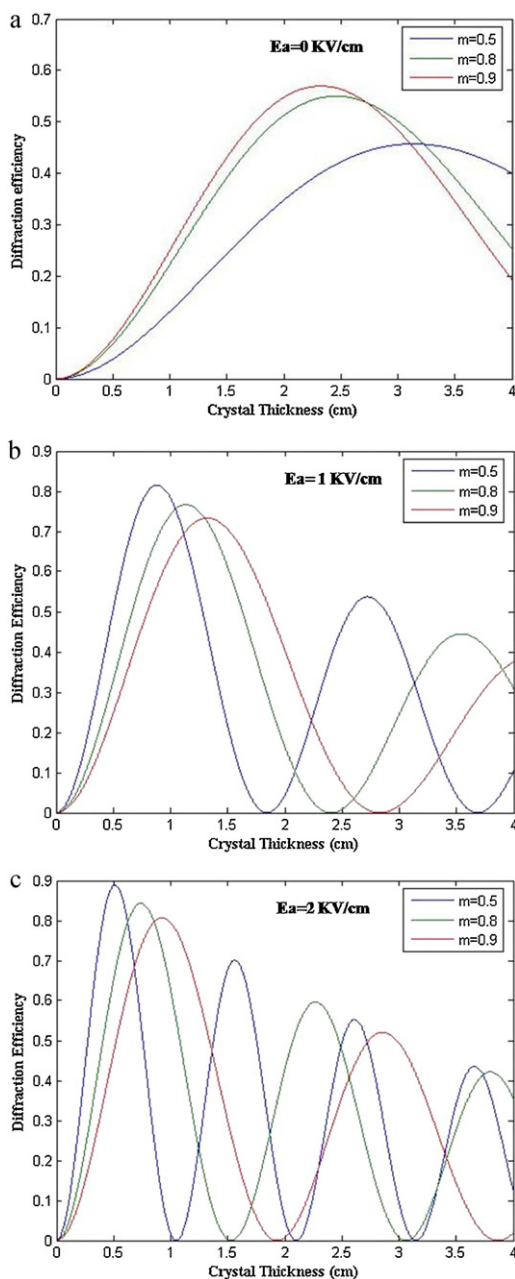


Fig. 2. Variation of diffraction efficiency with crystal thickness for different values of reduced fringe contrast modulation ratio with and without applied electric field.

enhanced under the application of the applied electric field. For an electric field of magnitude 1 kV/cm the diffraction efficiency is enhanced from 66% (without electric field Fig. 1(a)) to 80% (Fig. 1(b)) and for the applied electric field be 2 kV/cm it is 86% (Fig. 1(c)) and is different for different values of diffusion field.

Fig. 2(a)–(c) shows the plots of diffraction efficiency with crystal thickness for $E_d = 2$ kV/cm, $\theta_B = 28^\circ$, $K_g \cdot x = 3$, $\alpha = 0.2 \text{ cm}^{-1}$, $\lambda = 632.8 \text{ nm}$, $n_r = 2.41$, $r_{\text{eff}} = 28 \times 10^{-10}$ and for different values of reduced fringe contrast modulation ratio without applied electric field (Fig. 2(a)) and with the applied electric field (Fig. 2(b) and (c)). It is clear that the diffraction efficiency of the refractive index grating is higher for the higher values of reduced fringe contrast modulation ratio (without applied electric field). It is interesting to note here that under the application of external field the material response becomes reverse i.e. the diffraction efficiency of the index grating is found to be higher for the lower values of reduced fringe

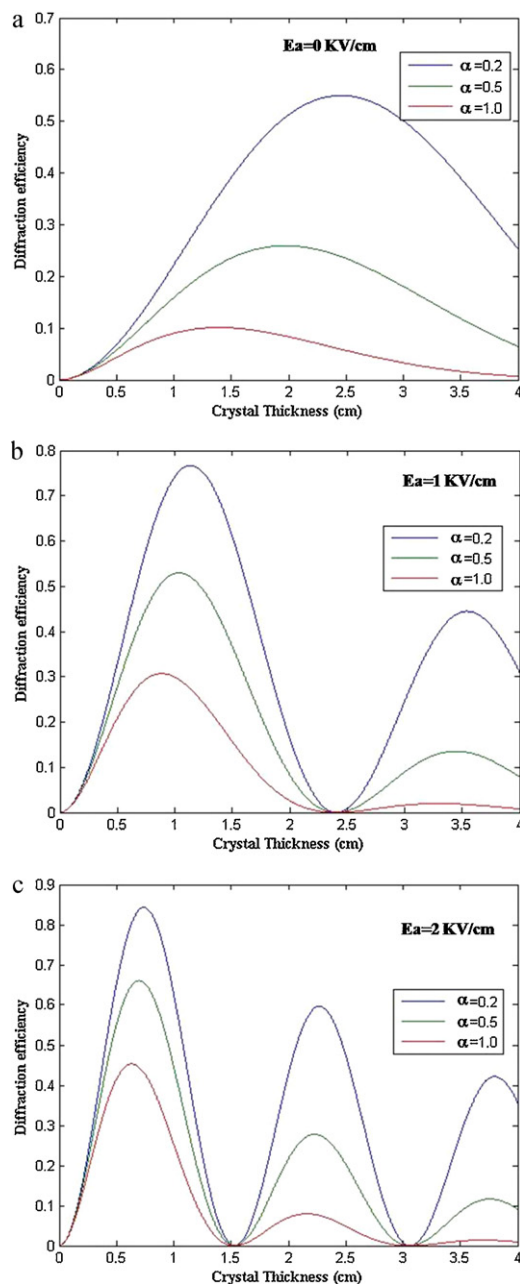


Fig. 3. Variation of diffraction efficiency with crystal thickness for different values of the absorption coefficient of the photorefractive materials with and without applied electric field.

contrast modulation ratio (Fig. 2(b) and (c)). From Fig. 1(a)–(c), one can see that the maximum diffraction efficiency of the index grating is shifted towards the lower values of crystal thickness as we increase the externally applied field. Diffraction efficiency can be raised by applying electric field. It increases from 46% to 80% when the applied field is increased from 0 to 1 kV/cm and it reaches to 90% when we apply an electric field of magnitude 2 kV/cm for the reduced fringe contrast modulation ratio $m = 0.5$ which is quite less than $m = 0.9$ [16].

In Fig. 3(a)–(c) we show the effect of the crystal thickness on the diffraction efficiency for a sample for $m = 0.8$, $\theta_B = 28^\circ$, $K_g \cdot x = 3$, $E_d = 2$ kV/cm, $\lambda = 632.8 \text{ nm}$, $n_r = 2.41$, $r_{\text{eff}} = 28 \times 10^{-10}$ and for different values of absorption coefficient. From these figures it is obvious that the diffraction efficiency of the index grating increases with crystal thickness and reaches to a maximum and afterwards it

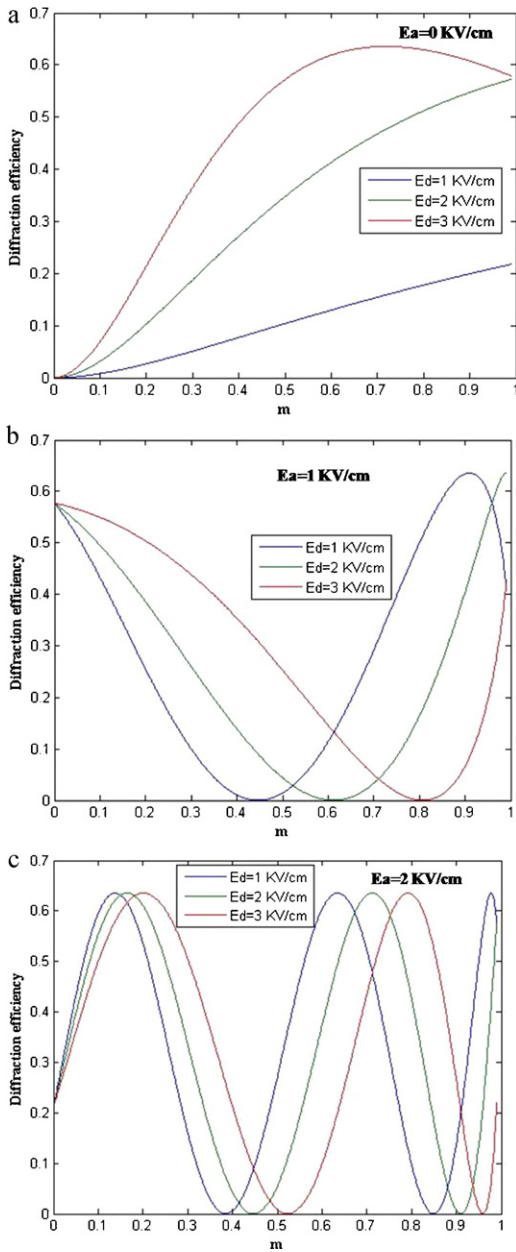


Fig. 4. Variation of diffraction efficiency with reduced fringe contrast modulation ratio for different values of diffusion field with and without applied electric field.

decreases and becomes minimum and again it increases and shows a periodic variation with the thickness of the material. It can be easily understood that the diffraction efficiency is lower for more absorbing materials. It is interesting to note that the maximum diffraction efficiency is observed at different crystal thicknesses for different values of absorption coefficient whereas its minimum is at the same crystal thickness for all values of absorption coefficient of the material. Further the maximum diffraction efficiency of the index grating is shifted towards the lower values of the crystal thickness for the higher values of absorption coefficient. The diffraction efficiency of the grating can be raised by applying external applied electric field. The second maximum of diffraction efficiency is observed with lower height to first maximum and the third maximum with lower height to the second maximum and so on due to the material absorption.

Variation of diffraction efficiency with reduced fringe contrast modulation ratio for $L=2$ cm, $\theta_B=28^\circ$, $K_g \cdot x=3$, $\alpha=0.2$ cm $^{-1}$,

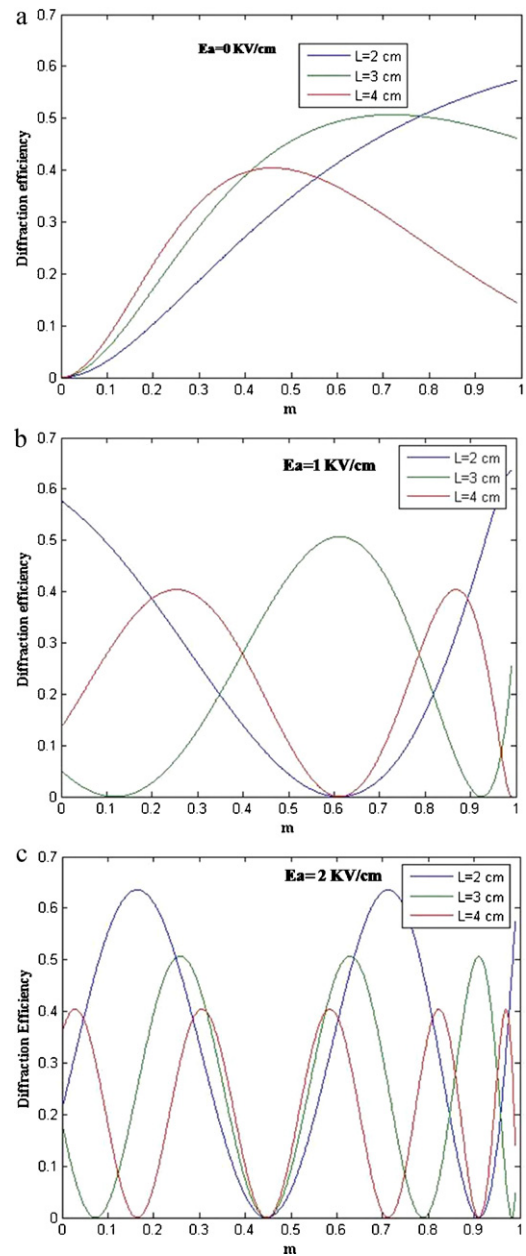


Fig. 5. Variation of diffraction efficiency with reduced fringe contrast modulation ratio for different values of crystal thickness of the materials with and without applied electric field.

$\lambda=632.8$ nm, $n_r=2.41$, $r_{eff}=28 \times 10^{-10}$ and for different values of diffusion field is shown in Fig. 4(a)–(c). It is evident from these figures that the diffraction efficiency increases with increasing reduced fringe contrast modulation ratio and is higher for higher values of diffusion field with constant diffusion field (without electric field) Fig. 4(a). With the external field one can see that higher diffraction efficiency is obtained at lower values of the reduced fringe contrast modulation ratio as compared to that without field. However, the magnitude of the diffraction efficiency maxima of the index grating is unaffected with the variation of applied electric field. It can also be seen that there is no change in the magnitude of diffraction efficiency with the diffusion field but the maxima and minima of the diffraction efficiency are observed at the lower values of the reduced fringe contrast modulation ratio for the lower values of diffusion field.

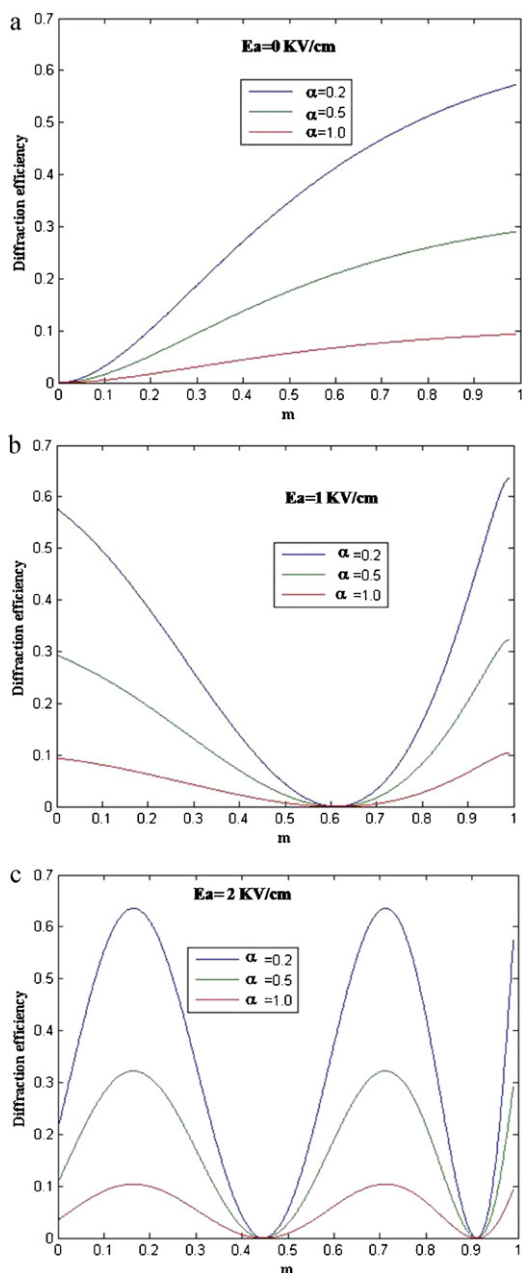


Fig. 6. Variation of diffraction efficiency with reduced fringe contrast modulation ratio for different values of absorption coefficient of the photorefractive materials with and without applied electric field.

Fig. 5(a)–(c) shows the plots of diffraction efficiency with the reduced fringe contrast modulation ratio for $E_d = 2$ kV/cm, $\theta_B = 28^\circ$, $K_g \cdot x = 3$, $\alpha = 0.2$ cm $^{-1}$, $\lambda = 632.8$ nm, $n_r = 2.41$, $r_{eff} = 28 \times 10^{-10}$ and for the photorefractive materials of different thicknesses and with the applied electric field. From these figures one can easily see that thinner material shows higher diffraction efficiency than that of thicker materials. If we apply an external field the maxima of the diffraction efficiency is observed at the lower values of m but the magnitude of the maximum diffraction efficiency remains unchanged with the applied. When the magnitude of the applied field is 1 kV/cm the minima of the diffraction efficiency is observed at the particular value of m for $L = 2$ cm and $L = 4$ cm whereas for $L = 3$ cm it shows maxima at that particular value of m . But for the applied field 2 kV/cm one of the minima's of the diffraction efficiency for $L = 2, 3$, and 4 cm observed at the same value of $m = 0.45$, not all but

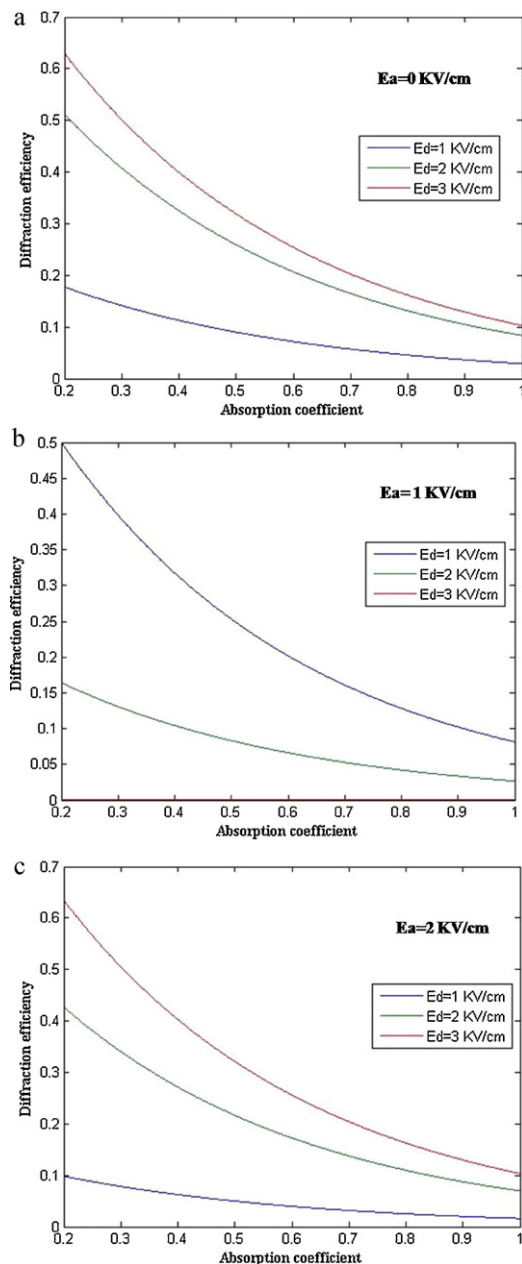


Fig. 7. Variation of diffraction efficiency with absorption coefficient of the photorefractive materials for different values of diffusion field with and without applied electric field.

maxima are different for different values of crystal thickness and are observed at different values of m .

Variation of diffraction efficiency with the reduced fringe contrast modulation ratio for $E_d = 2$ kV/cm, $\theta_B = 28^\circ$, $K_g \cdot x = 3$, $L = 2$ cm, $\lambda = 632.8$ nm, $n_r = 2.41$, $r_{eff} = 28 \times 10^{-10}$ and for different values of absorption coefficient is shown in Fig. 6(a)–(c) without and with externally applied electric field. A periodic variation is observed in diffraction efficiency with reduced fringe contrast modulation ratio. Efficiency is different for different values of absorption coefficient. The material having lower absorption coefficient shows higher diffraction efficiency. The maxima and minima of the diffraction efficiency are observed at the same value of m for any value of absorption coefficient. However, the maxima and minima are shifted towards the lower values of m for the higher values of applied external electric field [Fig. 6(a)–(c)].

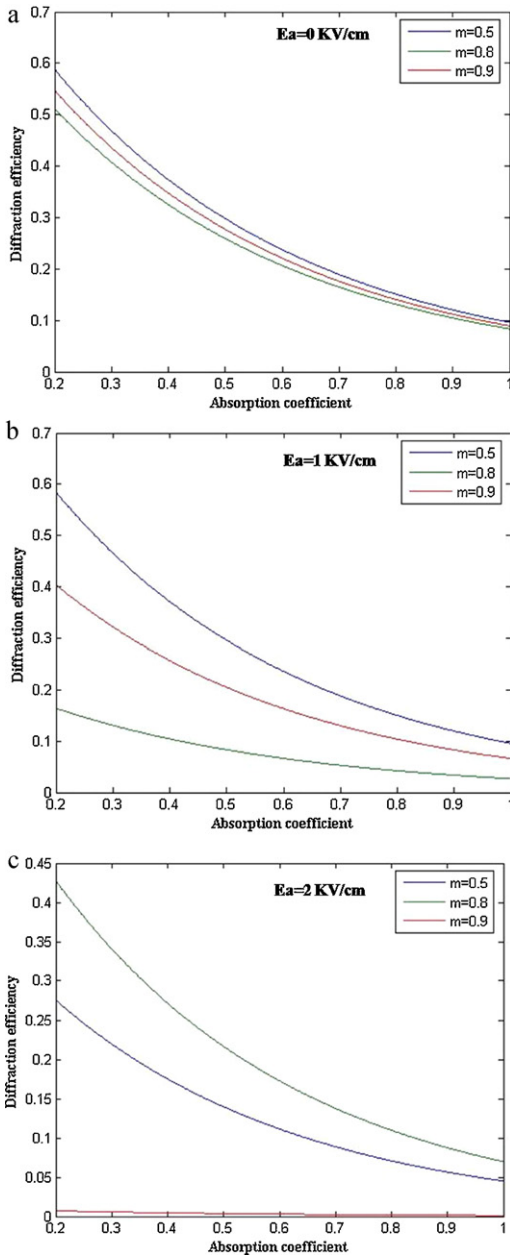


Fig. 8. Variation of diffraction efficiency with absorption coefficient of the photorefractive materials for different values of reduced fringe contrast modulation ratio with and without applied electric field.

Fig. 7(a)–(c) depicts the variation of diffraction efficiency as a function of absorption coefficient of the material for $m = 0.8$, $\theta_B = 28^\circ$, $K_g \cdot x = 3$, $L = \text{cm}$, $\lambda = 632.8 \text{ nm}$, $n_r = 2.41$, $r_{eff} = 28 \times 10^{-10}$ and for different values of diffusion field with and without the externally applied electric field. From these figures it is evident that the diffraction efficiency decreases with increasing absorption coefficient and it has different magnitudes for different values of diffusion field. Further, its magnitude is higher for higher values of diffusion field in the absence of field. On applying the electric field the efficiency is lower for higher diffusion field. When we apply electric field of magnitude 1 kV/cm, the observed diffraction efficiency is lower for higher values of diffusion field. However, in the case when the magnitude of the externally applied electric field is 2 kV/cm the magnitude of the diffraction efficiency is found to be higher for higher values of diffusion field. Thus, one can say that with the application of external electric field of

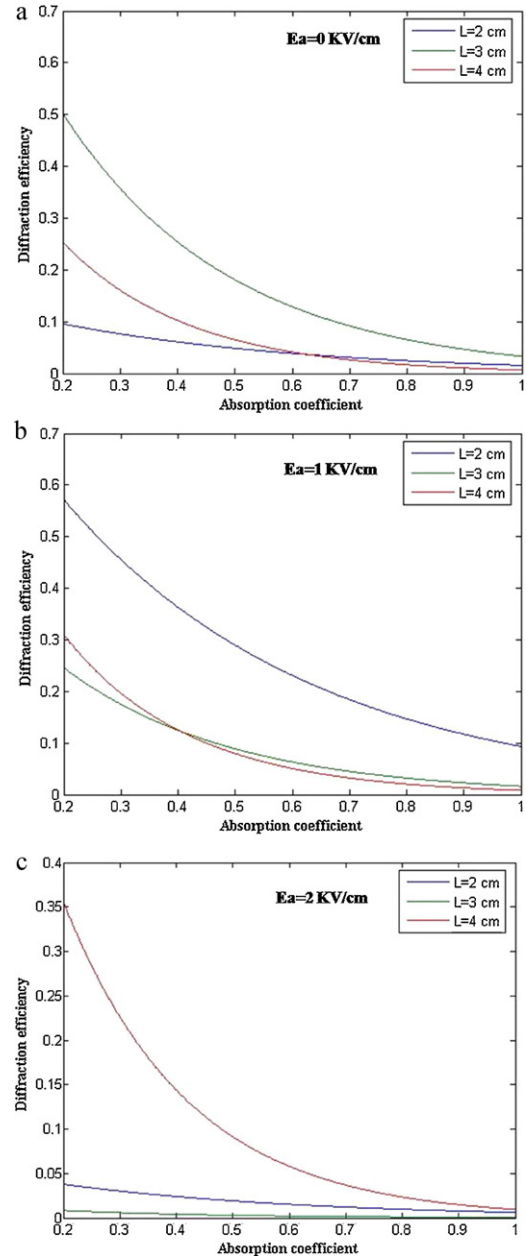


Fig. 9. Variation of diffraction efficiency absorption coefficient of the photorefractive materials for different values of crystal thickness of the materials with and without applied electric field.

magnitude 2 kV/cm the diffraction efficiency shows the reverse effect to that with the field of magnitude 1 kV/cm [Fig. 7(b)–(c)]. From Fig. 7(a)–(c) one may conclude that the diffraction efficiency of the holograms can be enhanced by applying the electric field of smaller magnitude ($E_a \leq 1$ kV/cm) which is possible for much lower value of diffusion field ($E_d \leq 1$ kV/cm) of the photorefractive material. This means that the diffraction efficiency of the hologram can be increased by applying lower magnitude of the electric field with the very small value of the diffusion field.

Variation of diffraction efficiency with absorption coefficient for $E_d = 2$ kV/cm, $\theta_B = 28^\circ$, $K_g \cdot x = 3$, $L = 2$ cm, $\lambda = 632.8 \text{ nm}$, $n_r = 2.41$, $r_{eff} = 28 \times 10^{-10}$ and for different values of reduced fringe contrast modulation ratio is shown in Fig. 8(a)–(c). From these figures it is clear that the diffraction efficiency decreases with the increasing absorption coefficient. Its magnitude is different for different

values of m but it is higher for lower values of m in absence of the applied field. When we apply electric field of magnitude 1 kV/cm, observed diffraction efficiency is lower for higher values of m but for lower values of m ($=0.5$) there is no change in the magnitude of the diffraction efficiency. But with external electric field of magnitude 2 kV/cm it shows the reverse effect of that in case of the external field of 1 kV/cm, i.e. for m ($=0.5$) the diffraction efficiency reduces from 59% to 27% and for m ($=0.9$) it increases from 18% to 43% while for $m=0.8$ it reduces to a minimum value. Thus, one may conclude that without electric field the diffraction efficiency of the hologram recorded in photorefractive media is better than that of the recorded in the presence of electric field.

Variation of diffraction efficiency with absorption coefficient for $m=0.8$, $E_d=2$ kV/cm, $\theta_B=28^\circ$, $K_g \cdot x=3$, $\lambda=632.8$ nm, $n_r=2.41$, $r_{eff}=28 \times 10^{-10}$ and for the materials of different thickness is shown in Fig. 9(a)–(c). It is evident from these figures that the diffraction efficiency decreases with the increasing absorption coefficient of the material and its magnitude is different for different values of crystal thickness but is higher for higher values of crystal thickness in the absence of the externally applied electric field. On applying the electric field of magnitude 1 kV/cm, diffraction efficiency is lower for higher values of crystal thickness. But with the external electric field of magnitude 2 kV/cm it shows the reverse effect to that in case of the externally applied electric field of 1 kV/cm. From Fig. 9(a)–(c) one may observe that the diffraction efficiency of holograms can be increased by increasing the crystal thickness of the photorefractive materials in the absence of the electric field whereas, in the presence of the electric field ($E_a \leq 1$ kV/cm) the diffraction efficiency of holograms can be enhanced by reducing the crystal thickness of the photorefractive materials.

4. Conclusion

The diffraction efficiency of a holographic index grating in photorefractive materials has been calculated by solving the material rate equations via the total space charge field. It is found that in the absence of externally applied electric field the diffraction efficiency of the grating is higher for the higher reduced fringe contrast modulation ratio. It is interesting to note here that under the application of externally applied electric field the response of the materials becomes opposite i.e. the diffraction efficiency of the index grating is found to be higher for the lower reduced fringe contrast modulation ratio and vice versa. Diffraction efficiency can be enhanced by applying external electric field. It can be enhanced up to 95% with a field of 20 kV/cm [16] but in the present case it can be enhanced from 46% (without field) up to 80% with the applied electric field of magnitude 1 kV/cm. It reaches to 90% for an electric field of 2 kV/cm (for the reduced fringe contrast modulation ratio $m=0.5$). With the application of the externally applied electric field more efficient holograms can be recorded at very low applied electric field (~ 1 kV/cm) which is very less than that used in the earlier work (20 kV/cm) [16].

Acknowledgement

Two of the authors (TKY and MKM) acknowledge the CSIR, New Delhi, India for the financial support in form of CSIR-SRF during the research period.

References

- [1] P. Gunter, J.P. Huignard, *Photorefractive Materials and Their Application*, vols. 1 and 2, Springer, Berlin, 1988 and 1989.
- [2] J.P. Wilde, L. Hesselnik, Electric-field-controlled diffraction in photorefractive strontium barium niobate, *Opt. Lett.* 17 (1992) 853–855.
- [3] K. Sayano, A. Yariv, R.R. Neurgaonkar, Order-of-magnitude reduction of the photorefractive response time in rhodium-doped $\text{Sr}_{0.6}\text{Ba}_{0.4}\text{Nb}_2\text{O}_6$ with a dc electric field, *Opt. Lett.* 15 (1990) 9–11.
- [4] J.E. Ford, J. Ma, Y. Fainman, S.H. Lee, Y. Taketomi, D. Bize, R.R. Neurgaonkar, Multiplex holography in strontium barium niobate with applied field, *J. Opt. Soc. Am. A* 9 (1992) 1183–1192.
- [5] R. De Vre, M. Jeganathan, J.P. Wilde, L. Hesselnik, Effect of applied electric fields on the writing and the readout of photorefractive gratings, *J. Opt. Soc. Am. B* 12 (1995) 600–614.
- [6] A. Kewitsch, M. Segev, A. Yariv, R.R. Neurgaonkar, Electric-field multiplexing/demultiplexing of volume holograms in photorefractive media, *Opt. Lett.* 18 (1993) 534–536.
- [7] A.V. Chamrai, M.P. Petrov, V.M. Petrov, Optical configuration for electric field multiplexing of volume holograms in photorefractive ferroelectrics, *OSA Trends Opt. Photon. (TOPS)* 27 (1999) 515.
- [8] J.P. Huignard, J.P. Herriau, P. Aubourg, E. Spitz, Phase-conjugate wavefront generation via real-time holography in $\text{Bi}_{12}\text{SiO}_{20}$ crystals, *Opt. Lett.* 4 (1979) 21–23.
- [9] A. Marrakchi, R.V. Johnson, A.R. J.Jr. Tranguay, Polarization properties of photorefractive diffraction in electrooptic and optically active sillenite crystals (Bragg regime), *J. Opt. Soc. Am. B* 3 (1986) 321–336.
- [10] J.M. Haeton, L. Solimar, Transient effects during dynamic hologram formation in BSO crystals: theory and experiment, *IEEE J. Quantum Electron.* 24 (1988) 558–567.
- [11] S.I. Stepanov, M.P. Petrov, Efficient unstationary holographic recording in photorefractive crystals under alternating electric field, *Opt. Commun.* 53 (1985) 292–295.
- [12] G. Pauliat, G. Roosen, Photorefractive effect generated in sillenite crystals by picosecond pulses and comparison with the quasi-comparison with the quasi-continuous regime, *J. Opt. Soc. Am. B* 7 (1990) 2259–2267.
- [13] A. Grunnet-Jepsen, I. Aubrecht, L. Solymar, Investigation of the internal field in photorefractive materials and measurement of the effective electro-optic coefficient, *J. Opt. Soc. Am. B* 12 (1995) 921–929.
- [14] A.A. Kamshilin, E.V. Mokrushina, M.P. Petrov, Adaptive holographic interferometers operating through selfdiffraction of recording beams in photorefractive crystals, *Opt. Eng.* 28 (1989) 580–585.
- [15] R.C. Troth, J.C. Dainty, Holographic interferometry using anisotropic self-diffraction in $\text{Bi}_{12}\text{SiO}_{20}$, *Opt. Lett.* 16 (1991) 53–55.
- [16] I. Casar, L.F. Magaña, Influence of fringe bending on the enhancement of the diffraction efficiency of bismuth silicate gratings recorded under strong modulation and applied electric fields, *J. Opt. Soc. Am. B* 20 (2003) 736–740.
- [17] E.A. García, I. Casar, L.F. Magaña, Optimization of the diffraction efficiency of $\text{Bi}_{12}\text{SiO}_2$ under strong modulation and applied electric fields, *J. Opt. Soc. Am. B* 17 (2000) 1961–1966.
- [18] T.J. Hall, R. Jaura, L.M. Connors, P.D. Foote, The photorefractive effect – a review, *Prog. Quantum Electron.* 10 (1985) 77–146.
- [19] P. Yeh, *Introduction to Photorefractive Nonlinear Optics*, John Wiley & Sons Inc., New York, 1993.
- [20] L. Solimar, D. JWebb, A. Grunnet-Jepsen, The physics and applications of photorefractive materials, in: *Oxford Series in Optical Imaging and Sciences*, Clarendon Press, Oxford, 1996.
- [21] H. Kogelnik, Coupled wave theory for thick hologram gratings, *Bell Syst. Tech. J.* 48 (1969) 2909–2947.